## COMMUNICATION

Check for updates

# Mechanochemical templated synthesis of mesoporous alumina-supported polyoxometalate catalysts toward selective oxidation of sulfides†

Kang Xia, [ID] [ab] Shengtai Hou, [ID] [ac] Qiang Niu, [ID] [d] Kosuke Suzuki [ID] [b] and Pengfei Zhang [ID] *[ae]

Polyoxometalates are important catalysts, but their low surface area and leaching in solutions present challenges. We developed a facile, green, solvent-free mechanochemical method to anchor polyoxometalates on mesoporous alumina. The resulting catalysts showed high activity, selectivity in sulfide oxidation, and reusability for at least seven cycles, achieving gram-scale reactions efficiently.

Polyoxometalates (POMs) are a type of anionic metal–oxygen cluster that exhibit unique properties depending on their structures and compositions,[1] and to date, they have abundant applications such as catalysis, energy conversion, coordination chemistry and materials science.[2] For example, silicotungstate **SiW10** ($[SiW_{10}O_{36}]^{8-}$) can facilitate epoxidation of olefins by using hydrogen peroxide ($H_2O_2$),[3] and decatungstate **W10** ($[W_{10}O_{32}]^{4-}$) can be used in direct arylation of electron-deficient alkenes and strong C–H bonds.[4] Compared to the homogeneous use of POM catalysts,[2d,e,3–5] the development of heterogeneous POM catalysts has attracted increasing attention in order to attain green and sustainable chemistry owing to their facile separation and reusability toward practical applications.[2d,e,6] Hence, immobilizing POMs onto proper supports is an essential approach,[6,7] to effectively increase the very low specific area of POMs ($1–10 m^2 g^{-1}$).[1]

With the development of supported POM catalysts in the past few decades,[8] mesoporous materials such as mesoporous silica and mesoporous alumina have recently attracted much attention owing to their high specific area, large pore volume, and excellent stability (Table S1,† entries 1–15).[9,10] To date, various strategies have been developed to prepare supported POM catalysts, such as sol–gel synthesis, hydrothermal synthesis, and impregnation methods.[9,10] However, conventional solution-based methods are faced with concerns about using excessive organic solvents, time-consuming procedures, and limitations to soluble monomers.[8–11] Hence, mechanochemical synthesis that can be performed at room temperature under solvent-free conditions with a short reaction time, appears as a feasible solution based on our recent engagement in ball-milling synthesis.[11d–g] Notably, considering the possible structural decomposition of POMs in aqueous media,[12] this solvent-free synthesis is anticipated to provide a universal tool for the design of POM-based materials for diverse applications.[13] However, it remains a key issue how to efficiently incorporate POMs (precursors) with mesoporous supports while attaining a highly dispersed state.

Herein, we reported a versatile synthesis for preparing mesoporous alumina-supported POM catalysts using a soft-template approach *via* mechanochemistry (Fig. 1). Notably, POMs themselves can function as cross-linking agents with the template and support through electrostatic interactions. A supported POM catalyst with a high specific area (up to 644 m²

*School of Chemistry and Chemical Engineering, Shanghai Jiao Tong University, Shanghai 200240, China. E-mail: chemistryzpf@sjtu.edu.cn*

*Department of Applied Chemistry, School of Engineering, The University of Tokyo, 7-3-1 Hongo, Bunkyo-ku, Tokyo 1138656, Japan*

*Hebei Key Laboratory of Close-to-Nature Technology of Wetlands, School of Eco-Environment, Hebei University, Baoding 071002, China*

*National Enterprise Technology Center, Inner Mongolia Erdos Electric Power and Metallurgy Group Co., Ltd, Ordos, Inner Mongolia 016164, China*

*State Key Laboratory of High-efficiency Utilization of Coal and Green Chemical Engineering, Ningxia University, Yinchuan 750021, China. E-mail: pfzhang@nxu.edu.cn*
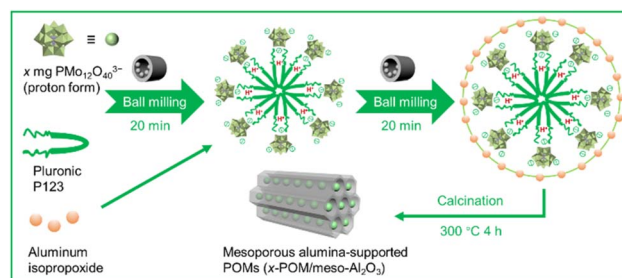
Fig. 1 Illustration for the preparation of *x*-POM/meso-Al₂O₃ catalysts *via* a mechanochemical templated synthesis.

$g^{-1}$) and narrow pore size distribution can be prepared within several hours, in comparison to the days of synthesis required by conventional methods (Table S1†). These catalysts efficiently performed the selective oxidation of sulfides with both the conversion rate of various sulfides and the selectivity of corresponding sulfoxides above 90%. Furthermore, this catalyst can be reused for at least 7 cycles without a noticeable decrease in activity or loss of POM components and can catalyze the reaction on a gram-scale, symbolizing an efficient heterogeneous catalyst.

Mesoporous alumina-supported POM catalysts with different loading amounts ($x$-POM/meso-Al$_2$O$_3$) were prepared by templated solvent-free mechanochemical synthesis, based on knowledge of nonhydrolytic sol–gel synthesis in which the condensation of chloride and aluminum alkoxides was utilized.[14] Hence, condensation between anionic POMs and cationic aluminum precursors with electrostatic interactions was realized. Specifically, POM **PM12** ($H_3PMo_{12}O_{40}$) and surfactant pluronic P123 were mixed by ball milling for 20 min, followed by the addition of aluminum isopropoxide (AIP) and ball milling for 20 min, and calcination at 300 °C for 4 h for removing organics to give the mesoporous alumina framework inside being doped with POMs as active sites for catalysis, labeled as $x$-POM/meso-Al$_2$O$_3$ (Fig. 1, $x$ mg of POMs corresponds to 2.04 g of AIP).

Notably, the calcination temperature was set at 300 °C to completely remove P123 and prevent thermal decomposition of POMs as plenary POMs including PM12 often remain stable below 350 °C.[15] Also, a heating rate of 1 °C min$^{-1}$ was adopted to prevent the collapse of the tunnels in mesoporous alumina. By varying the amount of P123, the usage of 1.0 g was confirmed to achieve the highest surface area of 483 m$^2$ g$^{-1}$ (Table S2,† entries 1–4). In the presence of **PM12**, a higher surface area of 570 m$^2$ g$^{-1}$ for alumina can be observed owing to the presence of **PM12** as a cross-linking agent for the sol–gel process (Table S2,† entries 5–8). The pre-treatment of AIP with grinding was found to be effective in increasing the surface area, and the addition sequence, as provided in Table S2†, led to a record-high surface area of 644 m$^2$ g$^{-1}$ for 100-**PM12**/meso-Al$_2$O$_3$(-Tables S1 and S2†).

Both 100-**PM12**/meso-Al$_2$O$_3$ and meso-Al$_2$O$_3$ obtained in the absence of POMs displayed typical type-V isotherms with H2-type hysteresis loops, indicating their mesoporous structure and piled pores (Fig. 2a),[16] in which the larger hysteresis loop for 100-**PM12**/meso-Al$_2$O$_3$ suggested a higher surface area than meso-Al$_2$O$_3$ (Table S2,† entries 4 and 10). The pore diameter distribution also proved the existence of mesoporous pores in the range of 2–8 nm (Fig. S1†), and a record-high pore volume of 0.487 cm$^3$ g$^{-1}$ for 100-**PM12**/meso-Al$_2$O$_3$ compared to that of reported supported POM catalysts (Table S1†). This result supported our hypothesis that POMs can be not only immobilized on the *in situ* formed mesoporous alumina support, but also can further increase the surface area and pore volume of the obtained composite by facilitating the nonhydrolytic sol–gel process (Fig. 1).

To explore the crystallinity of as-synthesized mesoporous composites, X-ray diffraction (XRD) was performed. By varying
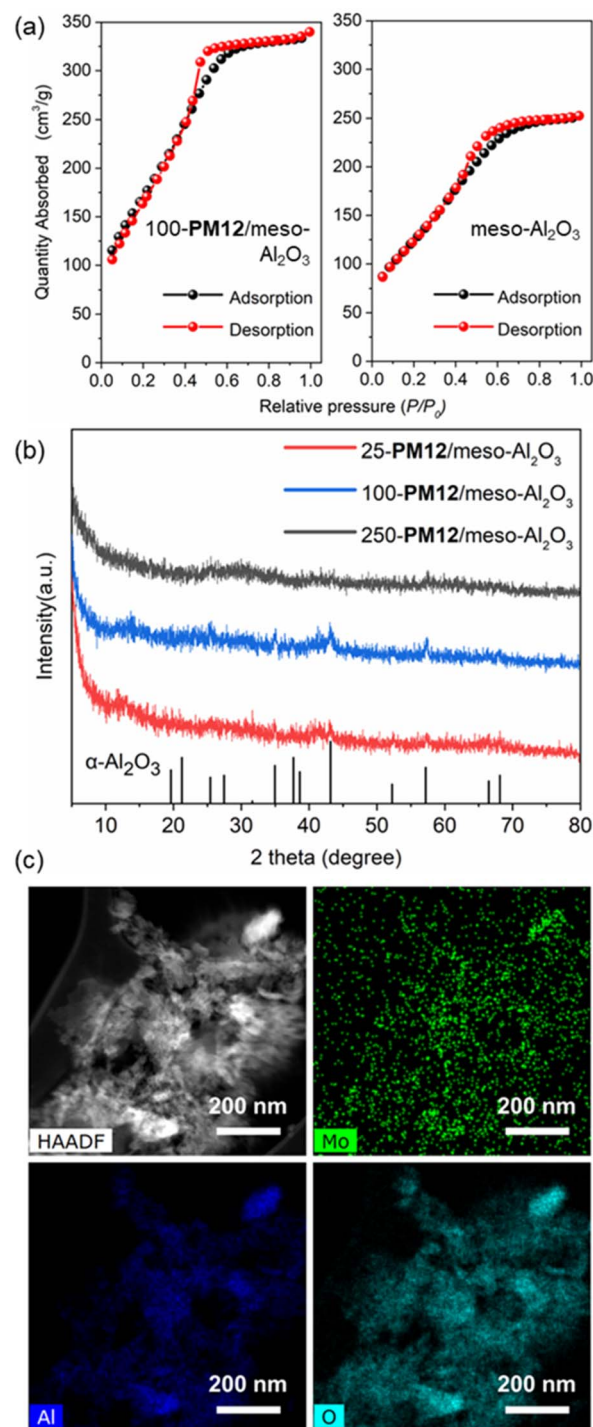


Fig. 2 (a) N$_2$ adsorption−desorption isotherms (77 K) of 100-**PM12**/meso-Al$_2$O$_3$ and meso-Al$_2$O$_3$; (b) XRD spectra of varying loading amounts of POMs as $x$-**PM12**/meso-Al$_2$O$_3$; (c) STEM EDS-mapping images of 100-**PM12**/meso-Al$_2$O$_3$.

the amount of loading amount of **PM12**, there existed weak peaks parallel to those of α-Al$_2$O$_3$, supporting the mesoporous nature of $x$-**PM12**/meso-Al$_2$O$_3$. Meanwhile, there existed no obvious peaks for **PM12** in the XRD spectra despite varying the amount of **PM12** (Fig. 2b). As **PM12** retained the main peak at

26° and other minor peaks with much decreased intensity after ball milling for 40 min (Fig. S2†), the absence of XRD patterns of POMs can be attributed to even mixing of POMs and $Al_2O_3$ into fine powders, leading to a high surface area and a relatively low supporting amount of **PM12** (16 wt% for 100-**PM12**/meso-$Al_2O_3$). The infrared (IR) spectra were recorded and despite overlapping of peaks with $Al_2O_3$ (Fig. S3†), the characteristic peaks of **PM12** at 1060 and 970 cm$^{-1}$ were retained, supporting the retained structures of POMs in x-**PM12**/meso-$Al_2O_3$.[17]

Scanning electron microscopy (SEM) analysis was further carried out, which revealed that by varying loading amounts of **PM12** from 25 mg, 100 mg (i.e., 100-**PM12**/meso-$Al_2O_3$) to 250 mg, the number of particles of catalysts dispersed on the matrix increased significantly, which indicated successful immobilization of **PM12** on meso-$Al_2O_3$ (Fig. S4†). However, the use of 250 mg of POMs led to the over-packing structure of 250-**PM12**/meso-$Al_2O_3$, indicating that a portion of the mesoporous pores was blocked according to BET results (Table S2,† entries 1–4). The high-angle annular dark field scanning TEM (HAADF-STEM) revealed the porous structure of 100-**PM12**/meso-$Al_2O_3$ and piled pores and tunnels with quite uniform distribution in diameters below 10 nm (Fig. S5†). Notably, the average pore diameter of 3.3 nm in STEM images was consistent with that in BET analysis, indicating the mesoporous pores (Fig. S1, S5a and b†). Furthermore, energy dispersive X-ray spectroscopy (EDS) was carried out to evaluate elemental composition for 100-**PM12**/meso-$Al_2O_3$. It was demonstrated that molybdenum, aluminum, and oxygen elements were evenly distributed, together with IR and XRD results indicating that **PM12** retained its structure and achieved a highly dispersed state on meso-$Al_2O_3$ (Fig. 2c and S6†). Based on the above characterization studies, we developed a non-solvent-based mechanochemical method for preparing supported POM catalysts with high surface area, mesoporous pores, and well-dispersed states within hours.

Selective oxidation of sulfides is an important process in the catalysis community with many applications that range from organic synthesis to industrial fine-chemical production.[18] Since POM-based materials have also been applied to a series of oxidation reactions,[1,2] in order to utilize the above-developed properties, we applied x-**PM12**/meso-$Al_2O_3$ to selective oxidation of sulfides taking thioanisole (**1a**) to methyl phenyl sulfoxide (**2a**) conversion as a representative reaction, with $H_2O_2$ as a green oxidant (Fig. S7 and S8†). First, the loading amount of POMs was evaluated, and the reaction proceeded to some extent with low selectivity in the absence of POMs (Table S3,† entries 1 and 2). By increasing the amount of POMs, the conversion increased up to 100 mg (i.e., 100-**PM12**/meso-$Al_2O_3$), and decreased when using 250 mg POMs with a decrease in selectivity for 250-**PM12**/meso-$Al_2O_3$, which can be attributed to the as-observed over-packing structure (Table S3 and Fig. S4†). Then, a higher amount of $H_2O_2$ was found to facilitate the over-oxidation of **1a** into methyl phenyl sulfone (**3a**), thus the same equivalent of $H_2O_2$ to **1a** was considered optimal (Table S4†). Furthermore, the effect of solvent on catalysis was evaluated, and both conversion and selectivity were significantly higher when using alcohol solvents than other solvents, which can be

attributed to the fact that protic solvent can provide protons in the catalytic system to enhance acid catalysis of POMs (i.e., 100-**PM12**/meso-$Al_2O_3$).[18d] The low activity when using toluene as the solvent was related to the fact that, on the one hand, solvents with low polarity impeded the dissolution of $H_2O_2$, decreasing the reaction rate, and on the other hand, they facilitated the formation of **3a** with lower polarity.

The substrate scope was further studied and x-**PM12**/meso-$Al_2O_3$ can facilitate selective oxidation of less reactive alkyl sulfides (**1e** and **1f**) or aryl sulfides (**1b**, **1c**, and **1d**) with electron-withdrawing groups (–F, –Cl, and –Br) to the corresponding sulfoxide products with high selectivity exceeding 90% (Fig. 3a). Moreover, x-**PM12**/meso-$Al_2O_3$ can be easily retrieved from the catalytic solution through high-speed centrifugation and can be reused for at least 7 times without a notable decrease in catalytic performance, while the conversion and the selectivity still retained at around 90% and 95%, respectively (Fig. 3b). There remained a transparent reaction solution for x-POM/meso-$Al_2O_3$ after catalysis compared to **PM12**, indicating few loss of POM components during the reaction (Fig. S9†). Subsequently,
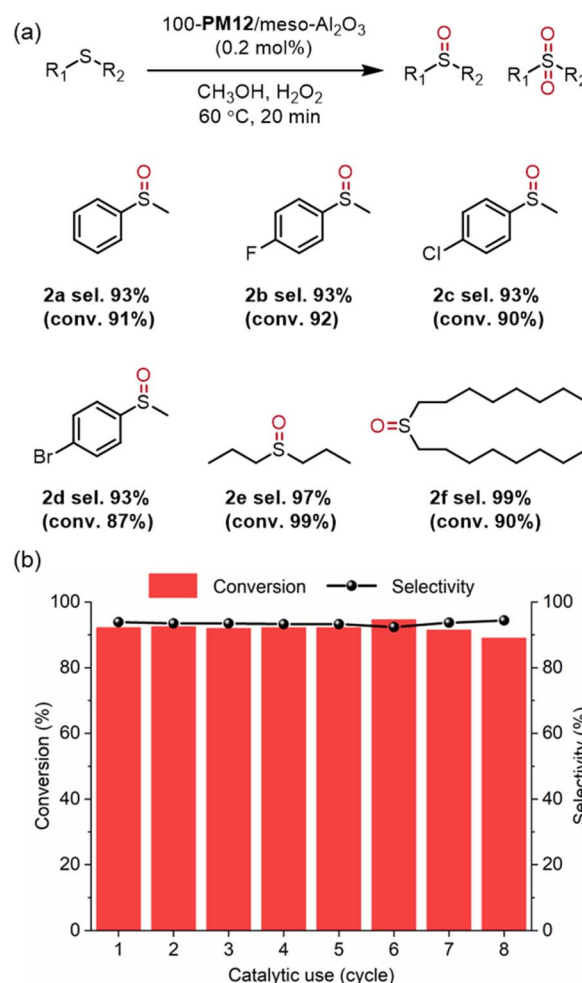


Fig. 3 100-**PM12**/meso-$Al_2O_3$-catalyzed selective oxidation of (a) different sulfide substrates; and (b) reused catalytic tests for selective oxidation of **1a**.

a gram-scale experiment with ten times the usage of thioanisole was performed using 100-**PMo12**/meso-Al$_2$O$_3$, and the conversion and the selectivity were 90% and 92%, respectively. The above results indicated that x-**PMo12**/meso-Al$_2$O$_3$ can be an efficient catalyst toward heterogeneous catalysis for industrial utilization.

In summary, we report a facile mechanochemical method for developing supported POM catalysts on mesoporous alumina at room temperature and under non-solvent conditions, completed within several hours. POMs can not only be immobilized on supports in a highly dispersed state but also contribute to achieving a high specific area (644 m$^2$ g$^{-1}$) and large pore volume (0.487 cm$^3$ g$^{-1}$), respectively. The obtained mesoporous composite can facilitate the selective oxidation of sulfides to sulfoxides with high activity and selectivity and can hold excellent durability toward reuse tests without activity loss for at least 7 cycles. We envisage that this synthetic methodology can provide a general strategy for developing POM-based materials especially based on the wide applicability of this method to different precursors (e.g., POMs, supports, and metal salts) and the avoidance of solvent usage to prevent general decomposition and isomerization of POMs.

## Data availability

The data supporting this article have been included as part of the ESI.†

## Conflicts of interest

There are no conflicts to declare.

## Acknowledgements

## Notes and references

1 (a) M. T. Pope, *Heteropoly and Isopoly Oxometalates*, Springer, 1983; (b) N. V. Izarova, M. T. Pope and U. Kortz, *Angew. Chem., Int. Ed.*, 2012, **51**, 9492; (c) H. N. Miras, J. Yan, D. L. Long and L. Cronin, *Chem. Soc. Rev.*, 2012, **41**, 7403.

2 (a) M. Sadakane and E. Steckhan, *Chem. Rev.*, 1998, **98**, 219; (b) H. Lv, Y. V. Geletii, C. Zhao, J. W. Vickers, G. Zhu, Z. Luo, J. Song, T. Lian, D. G. Musaev and C. L. Hill, *Chem. Soc. Rev.*, 2012, **41**, 7572; (c) M. Lechner, R. Güttel and C. Streb, *Dalton Trans.*, 2016, **45**, 16716; (d) I. A. Weinstock, R. E. Schreiber and R. Neumann, *Chem. Rev.*, 2018, **118**, 2680; (e) K. Suzuki, N. Mizuno and K. Yamaguchi, *ACS Catal.*, 2018,

**8**, 10809; (f) M. Anjass, G. A. Lowe and C. Streb, *Angew. Chem., Int. Ed.*, 2021, **60**, 7522.

3 K. Kamata, K. Yonehara, Y. Sumida, K. Yamaguchi, S. Hikichi and N. Mizuno, *Science*, 2003, **300**, 964.

4 (a) D. Dondi, M. Fagnoni, A. Molinari, A. Maldotti and A. Albini, *Chem.–Eur. J.*, 2004, **10**, 142; (b) I. Ryu, A. Tani, T. Fukuyama, D. Ravelli, M. Fagnoni and A. Albini, *Angew. Chem., Int. Ed.*, 2011, **50**, 1869; (c) I. B. Perry, T. F. Brewer, P. J. Sarver, D. M. Schultz, D. A. DiRocco and D. W. C. MacMillan, *Nature*, 2018, **560**, 70.

5 (a) I. A. Weinstock, *Chem. Rev.*, 1998, **98**, 113; (b) B. Keita and L. Nadjo, *J. Mol. Catal. A: Chem.*, 2007, **262**, 190; (c) S. He, Q. Liu and X. Wang, *J. Mater. Chem. A*, 2022, **10**, 5758.

6 (a) J. J. Stracke and R. G. Finke, *ACS Catal.*, 2014, **4**, 909; (b) M. Samaniyan, M. Mirzaei, R. Khajavian, H. Eshtiagh-Hosseini and C. Streb, *ACS Catal.*, 2019, **9**, 10174.

7 (a) Y. Zhou, G. Chen, Z. Long and J. Wang, *RSC Adv.*, 2014, **4**, 42092; (b) L. Lian, H. Zhang, S. An, W. Chen and Y. Song, *Sci. China:Chem.*, 2021, **64**, 1117.

8 (a) H. Li, N. Perkas, Q. Li, Y. Gofer, Y. Koltypin and A. Gedanken, *Langmuir*, 2003, **19**, 10409; (b) I. Tamiolakis, I. N. Lykakis, A. P. Katsoulidis, C. D. Malliakasc and G. S. Armatas, *J. Mater. Chem.*, 2012, **22**, 6919; (c) E. Skliri, I. N. Lykakis and G. S. Armatas, *RSC Adv.*, 2014, **4**, 8402; (d) A. Di, J. Schmitt, M. A. da Silva, K. M. Z. Hossain, N. Mahmoudi, R. J. Errington and K. J. Edler, *Nanoscale*, 2020, **12**, 22245; (e) K. Xia, T. Yatabe, K. Yonesato, T. Yabe, S. Kikkawa, S. Yamazoe, A. Nakata, K. Yamaguchi and K. Suzuki, *Angew. Chem., Int. Ed.*, 2022, **61**, e202205873; (f) K. Xia, T. Yatabe, K. Yamaguchi and K. Suzuki, *Dalton Trans.*, 2024, **53**, 11088.

9 (a) G. S. Armatas, A. P. Katsoulidis, D. E. Petrakisc and P. J. Pomonis, *J. Mater. Chem.*, 2010, **20**, 8631; (b) X. Yin, Z. Mei and Q. Yang, *J. Porous Mater.*, 2014, **21**, 729; (c) J. North, O. Poole, A. Alotaibi, H. Bayahia, E. F. Kozhevnikova, A. Alsalme, M. R. H. Siddiqui and I. V. Kozhevnikov, *Appl. Catal., A*, 2015, **508**, 16; (d) L. Hong, P. Win, X. Zhang, W. Chen, H. N. Miras and Y. Song, *Chem.–Eur. J.*, 2016, **22**, 11232; (e) Y. Liu, J. Chu, L. Lian, X. Chen, S. An, L. Hong, D. Wang and W. Chen, *Energy Fuels*, 2021, **35**, 2110.

10 (a) B. J. S. Johnson and A. Stein, *Inorg. Chem.*, 2001, **40**, 801; (b) M. Zhang, M. Li, Q. Chen, W. Zhu, H. Li, S. Yin, Y. Li and H. Li, *RSC Adv.*, 2015, **5**, 76048; (c) M. Craven, D. Xiao, C. Kunstmann-Olsen, E. F. Kozhevnikova, F. Blanc, A. Steiner and I. V. Kozhevnikov, *Appl. Catal., B*, 2018, **231**, 82; (d) F. Mirante, N. Gomes, L. C. Branco, L. Cunha-Silva, P. L. Almeida, M. Pillinger, S. Gago, C. M. Granadeiro and S. S. Baula, *Microporous Mesoporous Mater.*, 2019, **275**, 163; (e) J. Ortiz-Bustos, H. P. del Pulgar, Y. Pérez and I. del Hierro, *Dalton Trans.*, 2023, **52**, 10423.

11 (a) M. Klimakow, P. Klobes, A. F. Thünemann, K. Rademann and F. Emmerling, *Chem. Mater.*, 2010, **22**, 5216; (b) B. P. Biswal, S. Chandra, S. Kandambeth, B. Lukose, T. Heine and R. Banerjee, *J. Am. Chem. Soc.*, 2013, **135**, 5328; (c) M. Leonardi, M. Villacampa and J. C. Menéndez, *Chem. Sci.*, 2018, **9**, 2042; (d) P. Zhang, H. Li, G. M. Veith

and S. Dai, *Adv. Mater.*, 2015, **27**, 234; (*e*) P. Zhang, L. Wang, S. Yang, J. A. Schott, X. Liu, S. M. Mahurin, C. Huang, Y. Zhang, P. F. Fulvio, M. F. Chisholm and S. Dai, *Nat. Commun.*, 2017, **8**, 15020; (*f*) D. Chen, J. Zhao, P. Zhang and S. Dai, *Polyhedron*, 2019, **162**, 59; (*g*) Y. Shu, Q. Liu, M. Shi, Z. Zhang, C. Xie, S. Bi and P. Zhang, *Adv. Sci.*, 2024, **11**, 2304533.

12 N. I. Gumerova and A. Rompel, *Chem. Soc. Rev.*, 2020, **49**, 7568.

13 K. Xia, K. Yamaguchi and K. Suzuki, *Angew. Chem., Int. Ed.*, 2023, **62**, e202214506.

14 (*a*) W. Xiao, S. Yang, P. Zhang, P. Li, P. Wu, M. Li, N. Chen, K. Jie, C. Huang, N. Zhang and S. Dai, *Chem. Mater.*, 2018, **30**, 2924; (*b*) D. P. Debecker, V. Hulea and P. H. Mutin, *Appl. Catal., A*, 2013, **451**, 192.

15 (*a*) G. Mestl, T. Ilkenhans, D. Spielbauer, M. Dieterle, O. Timpe, J. Kröhnert, F. Jentoft, H. Knözinger and R. Schlögl, *Appl. Catal., A*, 2001, **210**, 13; (*b*) M. Ghali, C. Brahmi, M. Benltifa, C. Vaulot, A. Airoudj, P. Fioux, F. Dumur, C. Simonnet-Jégat, F. Morlet-Savary, S. Jellali, L. Bousselmi and J. Lalevée, *J. Polym. Sci.*, 2021, **59**, 153.

16 K. S. W. Sing, *Pure Appl. Chem.*, 1994, **66**, 1739.

17 C. Rocchiccioli-Deltcheff, M. Fournier, R. Franck and R. Thouvenot, *Inorg. Chem.*, 1983, **22**, 207.

18 (*a*) K. Sato, M. Hyodo, M. Aoki, X. Zheng and R. Noyori, *Tetrahedron*, 2001, **57**, 2469; (*b*) H. Egami and T. Katsuki, *J. Am. Chem. Soc.*, 2007, **129**, 8940; (*c*) E. Wojaczyńska and J. Wojaczyński, *Chem. Rev.*, 2010, **110**, 4303; (*d*) S. Hou, N. Chen, P. Zhang and S. Dai, *Green Chem.*, 2019, **21**, 1455.